Nanoscience and Nanometrology
2017; 3(2): 46-50
http://www.sciencepublishinggroup.com/j/nsnm
doi: 10.11648/j.nsnm.20170302.12
ISSN: 2472-3622 (Print); ISSN: 2472-3630 (Online)

Communication

Room-Temperature Si-Compatible Red Light Emission from In_2Se_3-Decorated Silicon Nanowires

Jinyou Xu

Key Laboratory of Advanced Micro/Nano Functional Materials, School of Physics and Electronic Engineering, Xinyang Normal University, Xinyang, The People's Republic of China

Email address:
Jinyou.xu@xynu.edu.cn

To cite this article:
Jinyou Xu. Room-Temperature Si-Compatible Red Light Emission from In_2Se_3-Decorated Silicon Nanowires. *Nanoscience and Nanometrology*. Vol. 3, No. 2, 2017, pp. 46-50. doi: 10.11648/j.nsnm.20170302.12

Received: June 19, 2017; **Accepted**: July 17, 2017; **Published**: August 9, 2017

Abstract: Next generation of Si-based nano-optoelectronic devices calls for monolithic integration of photonics with silicon. Here we report the synthesis of silicon nanowires with In_2Se_3 nanoflakes decorated by a one-step chemical vapor deposition under atmospheric pressure. These nanowires show pronounced red emission with wavelength in the range of 620-850 nm at room temperature under illumination of continuous wave laser. The strong emission originates from the photoluminescence of ultra-thin In_2Se_3 nanoflakes in view of the nanoscale footprint and atomically-thin thicknesses as well as high single-quality of the In_2Se_3 nanoflakes. This work demonstrated that nanoscale atomically-thin In_2Se_3 flakes can grow epitaxially on the surface of single-crystalline silicon nanowires and serves as strong red light emission centers for silicon nanowires. Therefore, these nanowires are promising to be used as a Si-compatible red light emission material for Si-based integrated nano-optoelectronic devices.

Keywords: Silicon Nanowires, Optical Materials and Properties, Luminescence, In_2Se_3

1. Introduction

The semiconductor of choice for the overwhelming majority of modern microelectronics, single-crystalline silicon (Si), is fundamentally unable to emit light due to its indirect bandgap. This fatal limitation has so far precluded the full integration of silicon microelectronics with photonics—which is expected to allow the realization of low-cost, high-speed optical information processing and communication in the future [1-4]. In this context, monolithic integration of optical emission with silicon structures has always been the subject active research, and one of the most urgent tasks is the design and fabrication of novel high-efficiency Si-compatible light emitting materials [5-7]. In fact, considerable progresses have been made in the last few years and several different approaches have been suggested. The underline mechanisms of these approaches can be classified into two categories. One entails direct approaches, including the dislocation-engineering [1, 4], the quantum confinement effect in silicon quantum dots and porous silicon [3], and the Raman laser of silicon [2, 8-10]. The other comprises indirect approaches, which mainly includes Si-based core-shell structures and rare earth doped silicon nanostructures. The former achieves emission by *in situ* grow emitting materials on the surfaces of silicon structure, for instance, Si-CdSSe core-shell nanowires emitted strong tunable visible light have been reported by Pan *et al* [5]. The later integrates the emission of rare earth ions into silicon nanostructures [11]. However, it's usually difficult to *in situ* grow semiconductor materials on silicon due to the large lattice-mismatch between them [5], while the rare earth doped silicon nanostructures seriously limited by the low ion concentrations [12].

In recent years, atomically-thin layered transition metal dichalcogenides have been attracted tremendous attention for their ability to enable light emission, which, however, is fundamentally forbidden for their bulk counterparts [13-16]. Indium selenide (In_2Se_3), with a narrow direct bandgap of 1.3-2.1 eV [17-19] and a hexagonal layered structure, is

considered as a promising candidate for lots of applications, such as photovoltaic solar cells [20], ionic batteries [21], phase change memory devices [22], visible-light photodetectors [23, 24] and field-effect transistors [25], benefited from its unique properties, such as efficient absorption, high sensitivity, polymorphism, large anisotropy of electrical properties and metal-ion defect structure [26, 27]. There are at least five known crystalline forms (α, β, γ, δ, κ) of In_2Se_3 existing at various temperatures, and the two common forms are α-phase and β-phase. Both them possess a layered crystallographic structure, usually crystallizes into double layers of nonmetal atoms [23, 25, 27], each consisting of the [Se-In-Se-In-Se] sheets stacked together through the Se atoms along the c-axis, as shown in Fig. 1a. What' worth noted

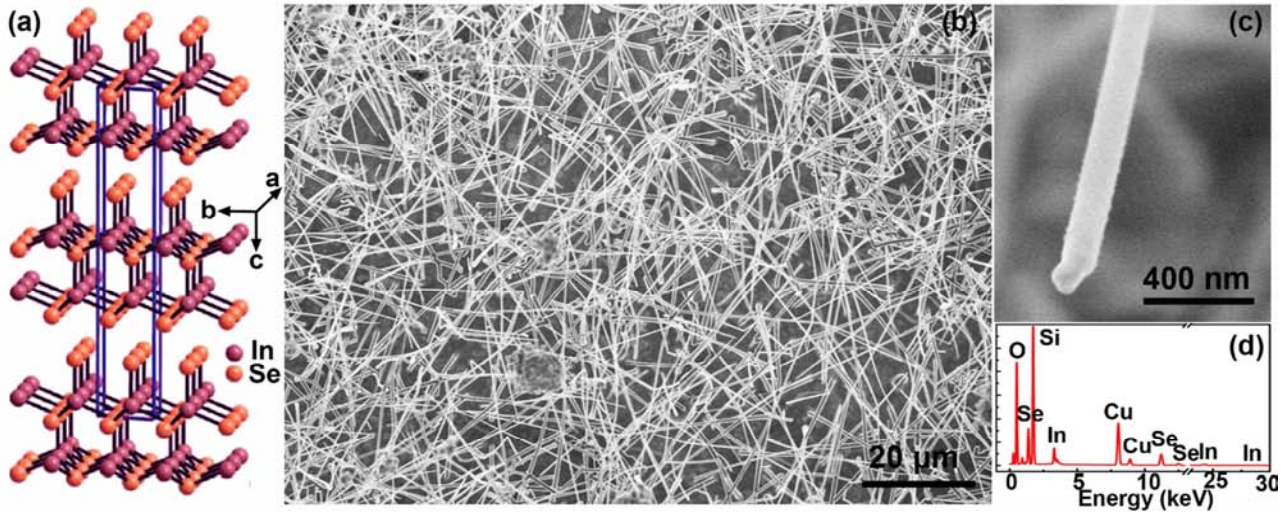

Figure 1. *(a) Atomic model of In_2Se_3 layered structure. (b, c) SEM of as-grown nanowires. (d) EDS collected from single nanowire dispersed on a cupper foil.*

is that the photoluminescence (PL) of In_2Se_3, has rarely been reported, although the layer structure and device applications of In_2Se_3 have been intensively investigated [19, 28, 29], In general, bulk and one-dimensional In_2Se_3 nanostructures show a ultra-low emission efficiency due to the existence of defects [19] and their excellent light absorption ability [29, 30].

In this work, we reported the epitaxial growth of ultra-thin In_2Se_3 nanoflakes on silicon nanowires by a one-step chemical vapor deposition (CVD) method. What's more important is that strong red PL from these In_2Se_3 nanoflakes was observed at room temperature for the first time. Furthermore, this PL was integrated into silicon nanowires, making these nanowires a competitive candidate as Si-compatible red light emitting material for Si-based nanophotonic applications.

2. Experimental Details

In_2Se_3-nanoflakes-decorated silicon nanowires were synthesized by a one-step CVD route. In a typically synthesis, 0.28 g silicon, 0.24 g selenium and 0.23 g indium powders (Alfa Aesar, 99.999%) were manually grated together before placed onto a ceramic boat located at the center of a quartz tube (Φ25×1000 mm) in a horizontal furnace. One piece of Au-coated Si wafer (1×2 cm^2) was placed at the downstream of the gas flow for sample deposition. N_2 gas was introduced for 1 hour to purge the O_2 inside the tube prior to heat. The furnace was then ramped to 900°C within 15 minutes and maintained at this temperature for another 1 hour.

The structural information of the as-prepared sample was characterized by scanning electron microscope (SEM, Hitachi S-4800), X-ray energy-dispersive spectrum (EDS) and transmission electron microscope (TEM, FEI Tecnai F20). The photoluminescent (PL) spectra of individual wire were performed on a confocal micro-PL system (Horiba, LabRAM HR Evolution) using a 532 nm laser as excitation source.

3. Results and Discussion

Typical SEM image in Fig. 1b shows the as-prepared wires possess uniform diameters of 100-200 nm, and a length of several tens of micrometers. Closing examination by high-magnification SEM image reveals the surfaces of these nanowires are not very clean, as shown in Fig. 1c. In addition, catalysts can be found on the tip of this nanowire, indicating the vapor-liquid-solid growth mechanism firstly established by Wagner [31]. The EDS recorded from single wire exhibits a strong Si peak and weak In, Se and O peaks, and the atomic ratio of In and Se is close to the 2:3 stoichiometry (not shown here). In addition, Cu peaks originate from the copper foil used for SEM observation were observed.

TEM characterization was carried out in order to investigate the microstructural details of these nanowires. Fig. 2a displays the morphology of the checked nanowires with uniform widths of ~200 nm. High-resolution TEM (HRTEM) image taken from the edge of the wire (Fig. 2b) clearly shows some crystal flakes (indicated with yellow arrows) with diameters of 4~10 nm decorated onto a single-crystalline nanowire. Enlarged examination from the selected area (dashed rectangle) further reveals that the crystal flakes possess two different orientations, and the angle between them is fixed to 109.5°, as shown in Fig. 2c. The lattice spacing of the wire trunk is 0.31 nm, in agreement with the (111) lattice plane of

cubic silicon (JCPDS No. 00-027-1402), while the most obvious periodicity of alternating bright and dark fringes of the crystal flakes are the same as 0.96 nm, in agreement with (002) lattice plane of layer-structured hexagonal α-In_2Se_3 (JSPDS No. 00-034-1279) [26]. Careful analyses reveal the selected area electron diffraction (SAED) image in Fig. 2d consists of three well-defined single sets of diffraction spots, demonstrating both the silicon trunk and the flakes are of high-quality single crystalline materials. Combining the EDS and HRTEM characterizations, those brighter spots (partially indicated with blue spots) was identified to be the SAED pattern of cubic silicon, while the other darker spots consistent to two SAED patterns of α-In_2Se_3 with the same arrangement but different orientations (partially indicated with green and red spots, respectively). It is worth noting that the angle between them is also fixed to 109.5° (indicated with white color), the same as what observed in the HRTEM, which further confirms the above deduce. Therefore, we are confident that the obtained nanowires are single crystal silicon nanowires decorated with lots of nanoscale size α-In_2Se_3 crystal flakes. This results is reasonable considering α-In_2Se_3 favors a layer structure and different layers was bonded together by weak van der Waals forces [18, 23, 25, 27] (Fig. 1a), and the spacing of (002) atomic plane of In_2Se_3 is exactly three times larger than the spacing of (111) lattice spacing of cubic silicon.

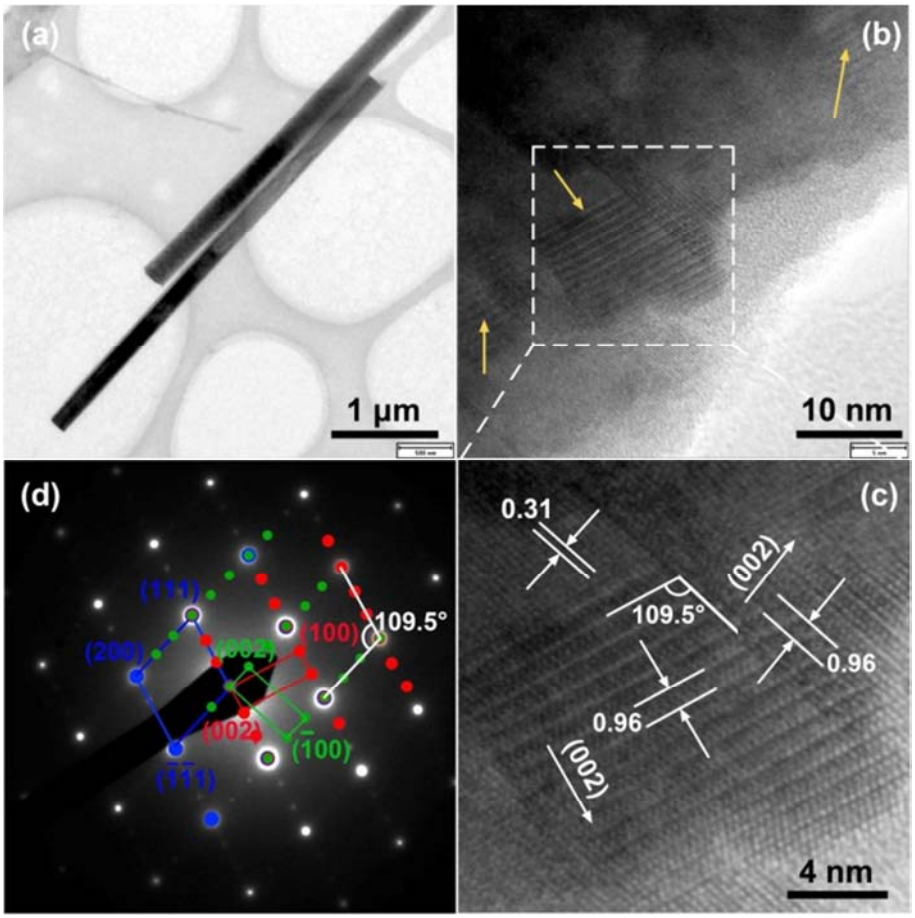

Figure 2. *(a) TEM. (b) HRTEM. (c) Enlarged image of the dashed rectangle area in panel b. (d) SAED of the wire in panel a, the green and red dots partially indicate two single sets of diffraction spots from hexagonal In_2Se_3, while the blue dots partially indicate the single set of diffraction spots from single-crystalline silicon.*

Interestingly, most of these special nanowires can emit strong red light at room temperature, even visible to human naked eyes, under the excitation of a diffused continuous wave laser (532 nm from a doubled Nd laser) with low power density (~50 mW/cm^2), as shown in Fig. 3a, 3b. When the laser beam was focused to a spot with diameters of ~5 microns (1 mW) by objective lens (Nikon, ×100), dazzling sparkle was observed from single nanowire, as shown in Fig. 3c, 3d. These results demonstrate the high emission efficiency of these nanowires. Fig. 3e gives the normalized room-temperature PL spectra collected from as-grown wires and single wire by the spectrometer equipped on the confocal micro-PL system (Horiba, LabRAM HR Evolution). As can be seen, the emission wavelengths cover from 620 nm (2.0 eV) to 850 nm (1.45 eV) with peak positions at around 720 nm. Since silicon is fundamentally unable to emit light [1-4] and the emitted photonic energy is in the range of the bandgap energy of bulk In_2Se_3 [17, 18], the obtained pronounced red light definitely comes from the In_2Se_3 nanoflakes epitaxially grown onto the surface of silicon nanowires. The 230 nm broad emission band might be attributed to the thermal fluctuation of energy levels [27-29] and the quantum confinement effect [7] inducted by

the broad size distribution of these nanoscale thin crystalline flakes, as confirmed by the HRTEM observations in Fig. 2. Since defect in In_2Se_3 is one of the main reasons that quenching its PL [19], the observation of strong room-temperature PL here further confirms the high single-crystal quality of the In_2Se_3 nanoflakes.

In general, bulk and one-dimensional nanostructured In_2Se_3 shows a ultra-low emission efficiency due to the existence of defects [19] and their excellent light absorption ability [29, 30]. However, here we find In_2Se_3 flakes emit pronounced light even under excitation of a diffused laser with low power density, which indicates the efficiency is comparable to CdS and CdSe nanowires that featured with a high PL efficiency [32]. Possible reasons for this high efficiency include the nanoscale sizes and atomically-thin thicknesses [33-35] as well as high crystalline quality of these nanoflakes (lack of defects) [19]. Very recently, Liu's group reported the first observation of PL signal with peak energy at 1.55 eV in atomic-layered α-In_2Se_3 fabricated by a physical evaporation [19]. They also found the PL intensity of In_2Se_3 is thickness-dependent, and PL quenched rapidly for few layered In_2Se_3. In addition, it's well known that semiconductor nanowires possess low luminescence quantum efficiencies, especially compared to their zero-dimensional analogue, namely, nanocrystals [33-35]. The underline mechanism have been recently clarified using pump-probe ultrafast spectroscopy by Lippitz et al [36]. They have demonstrated that about 10% of all absorbed photons lead to an excitation of the lowest energy state by measuring the transient absorption spectra of individual CdSe nanowires. Of these excitations, less than 1% emitted photons can reach the optical far-field, leading to an effective emission. In other words, almost all emission is reabsorbed by the other parts of the nanowire. This is in contrast to nanocrystals, where few absorbing states are in the close environment of the emitter. Therefore, the emission efficiency of nanocrystals and atomically thin layers generally is much higher compared with their bulk and one dimensional nanostructured analogues. For instance, bulk transition metal dichalcogenides have no PL at all at room temperature, but few-layered transition metal dichalcogenides, received intensive attention in recent years and are promising to be served as alternative of grapheme [14, 15], show significant PL at room temperature.

4. Conclusions

In summary, ultra-thin In_2Se_3 nanoflakes were epitaxially grown on the surface of silicon nanowires through a one-step CVD route. Due to the nanoscale sizes, atomically-thin thickness and high single-crystalline quality of these flakes, pronounced red photoluminescence with wavelength spanning from 620 nm to 850 nm was detected at room temperature, which has rarely been detected in bulk and few layered In_2Se_3. Furthermore, this strong photoluminescence was successfully integrated into single-crystalline silicon nanowires for the first time, hence achieved a high efficiency Si-compatible red light emitting, making them promising candidate for Si-based integrated optoelectronic devices and systems.

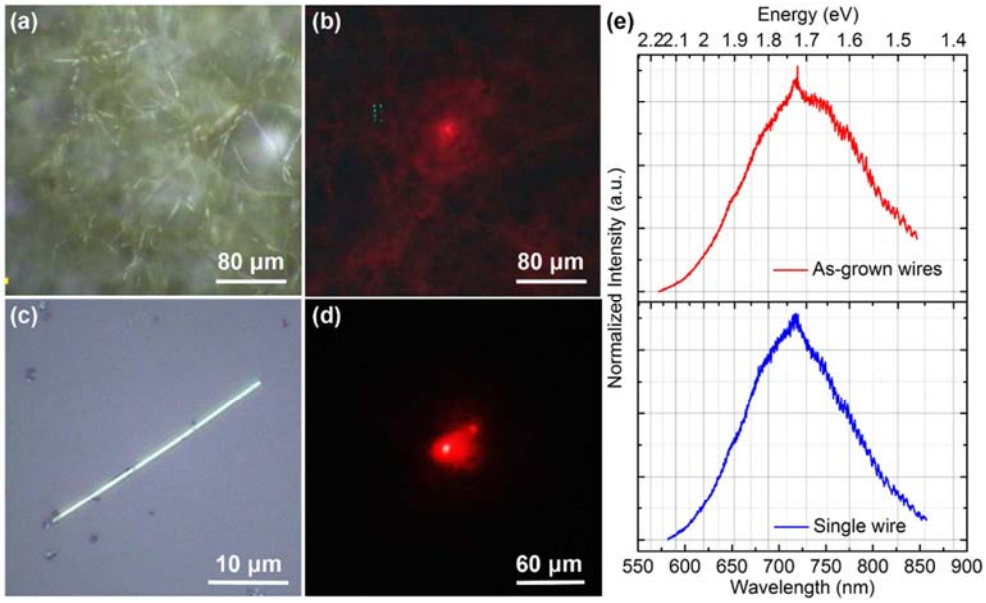

Figure 3. *Bright-field optical micrograph of as-grown nanowires (a) and dispersed single nanowire (c). Corresponding emission micrographs under excitation of a diffused (b) and focused (d) 532 nm laser, respectively. (e) Normalized PL spectra, red for the as-grown nanowires and blue for the single nanowire.*

Acknowledgements

The authors are grateful to the National Natural Science Foundation of China (Nos. 61504116), Nan Hu Young Scholar Supporting Program of XYNU, Research projects of Natural Science Foundation of Henan Province (No. 152300410124) and Youth Sustentation Fund of Xinyang Normal University (No.2014-QN-049), Program Projects of Science and Technology Innovative Research Team of Henan Province (18IRTSTHN017) for financial support.

References

[1] Homewood, K. and Lourenco, M; Light from Si via dislocation loops. *Mater. Today*. 2005, *1*, 34-39.

[2] Rong, H; Liu, A; Jones, R; *et al;* An all-silicon Raman laser. *Nature*. 2005, *7023*, 292-294.

[3] Qu, Y. Q; Liao, L; Li, Y. J; *et al;* Electrically Conductive and Optically Active Porous Silicon Nanowires. *Nano Lett.* 2009, *12*, 4539-4543.

[4] Lourenço, M. A; Milosavljević, M; Gwilliam, R. M; *et al;* On the role of dislocation loops in silicon light emitting diodes. *Appl. Phys. Lett.* 2005, *20*, 201105.

[5] Zhou, W; Pan, A; Li, Y; *et al;* Controllable Fabrication of High-Quality 6-Fold Symmetry- Branched CdS Nanostructures with ZnS Nanowires as Templates. *J. Phys. Chem. C*. 2008, *25*, 9253-9260.

[6] Choi, H.-J; Shin, J. H; Suh, K; *et al;* Self-Organized Growth of Si/Silica/Er_2Si2O_7 Core−Shell Nanowire Heterostructures and their Luminescence. *Nano Lett.* 2005, *12*, 2432-2437.

[7] Xu, J; Li, H; Zhuang, X; *et al;* Synthesis and optical characterizations of chain-like Si@$SiSe_2$ nanowire heterostructures. *Nanoscale*. 2012, *5*, 1481-1485.

[8] Boyraz, O. and Jalali, B; Demonstration of a silicon Raman laser. *Opt. Express*. 2004, *21*, 5269-5273.

[9] Espinola, R; Dadap, J; Osgood Jr, R; *et al;* Raman amplification in ultrasmall silicon-on-insulator wire waveguides. *Opt. Express*. 2004, *16*, 3713-3718.

[10] Claps, R; Dimitropoulos, D; Han, Y; *et al;* Observation of Raman emission in silicon waveguides at 1.54 μm. *Opt. Express*. 2002, *22*, 1305-1313.

[11] Xu, J; Guo, P; Zou, Z; *et al;* Eu-doped Si-SiO_2 core–shell nanowires for Si-compatible red emission. *Nanotechnology*. 2016, *39*, 395703.

[12] Kenyon, A; Recent developments in rare-earth doped materials for optoelectronics. *Prog. Quant. Electron.* 2002, *4-5*, 225-284.

[13] Duan, X; Wang, C; Pan, A; *et al;* Two-dimensional transition metal dichalcogenides as atomically thin semiconductors: opportunities and challenges. *Chem. Soc. Rev.* 2015.

[14] Duan, X; Wang, C; Shaw, J. C; *et al;* Lateral epitaxial growth of two-dimensional layered semiconductor heterojunctions. *Nat. Nanotechnol*. 2014.

[15] Li, H; Duan, X; Wu, X; *et al;* Growth of Alloy $MoS_{2x}Se_{2(1–x)}$ Nanosheets with Fully Tunable Chemical Compositions and Optical Properties. *J. Am. Chem. Soc.* 2014, *10*, 3756-3759.

[16] Mak, K. F. and Shan, J; Photonics and optoelectronics of 2D semiconductor transition metal dichalcogenides. *Nat Photon*. 2016, *4*, 216-226.

[17] Sun, X. H; Yu, B; Ng, G; *et al;* III-VI compound semiconductor indium selenide (In_2Se_3) nanowires: Synthesis and characterization. *Appl. Phys. Lett*. 2006, *23*, 233121.

[18] Jacobs-Gedrim, R. B; Shanmugam, M; Jain, N; *et al;* Extraordinary Photoresponse in Two-Dimensional In_2Se_3 Nanosheets. *ACS Nano*. 2013, *1*, 514-521.

[19] Zhou, J; Zeng, Q; Lv, D; *et al;* Controlled Synthesis of High-Quality Monolayered α-In_2Se_3 via Physical Vapor Deposition. *Nano Letters*. 2015, *10*, 6400-6405.

[20] Lakshmikumar, S. and Rastogi, A; Selenization of Cu and In thin films for the preparation of selenide photo-absorber layers in solar cells using Se vapour source. *Sol. Energy Mater. Sol. Cells*. 1994, *1*, 7-19.

[21] Julien, C; Hatzikraniotis, E; Chevy, A; *et al;* Electrical behavior of Lithium intercalated layered In-Se compounds. *Mater. Res. Bull.* 1985, *3*, 287-292.

[22] Yu, B; Ju, S; Sun, X; *et al;* Indium selenide nanowire phase-change memory. *Appl. Phys. Lett.* 2007, *13*, 133119-133119-133113.

[23] Zhai, T. Y; Fang, X. S; Liao, M. Y; *et al;* Fabrication of High-Quality In_2Se_3 Nanowire Arrays toward High-Performance Visible-Light Photodetectors. *ACS Nano*. 2010, *3*, 1596-1602.

[24] Almeida, G; Dogan, S; Bertoni, G; *et al;* Colloidal Monolayer β-In2Se3 Nanosheets with High Photoresponsivity. *J. Amer. Chem. Soc*. 2017, *8*, 3005-3011.

[25] Lin, M; Wu, D; Zhou, Y; *et al;* Controlled Growth of Atomically Thin In_2Se_3 Flakes by van der Waals Epitaxy. *J. Amer. Chem. Soc*. 2013, *36*, 13274-13277.

[26] Peng, H. L; Xie, C; Schoen, D. T; *et al;* Large anisotropy of electrical properties in layer-structured In2Se3 nanowires. *Nano Lett*. 2008, *5*, 1511-1516.

[27] Ye, J; Soeda, S; Nakamura, Y; *et al;* Crystal Structures and Phase Transformation in In_2Se_3 Compound Semiconductor. *Jpn. J. Appi. Phys. Vol*. 1998, *8 Pt 1*, 4264-4271.

[28] Sánchez-Royo, J. F; Segura, A; Lang, O; *et al;* Optical and photovoltaic properties of indium selenide thin films prepared by van der Waals epitaxy. *J. Appl. Phys*. 2001, *6*, 2818-2823.

[29] Yang, M. D; Hu, C. H; Shen, J. L; *et al;* Hot Photoluminescence in gamma-In2Se3 Nanorods. *Nanoscale Res. Lett*. 2008, *11*, 427-430.

[30] Yang, M; Hu, C; Tong, S; *et al;* Structural and optical characteristics of γ-In_2 Se_3 Nanorods grown on Si substrates. *J. Nanomater.* 2011, 7.

[31] Wagner, R. and Ellis, W; Vapor-Liquid-Solid Mechanism of Single Crystal Growth. *Appl. Phys. Lett.* 1964, 89-90.

[32] Xu, J; Ma, L; Guo, P; *et al;* Room-Temperature Dual-Wavelength Lasing from Single-Nanoribbon Lateral Heterostructures. *J. Amer. Chem. Soc.* 2012, *30*, 12394-12397.

[33] Puthussery, J; Lan, A; Kosel, T. H; *et al;* Band-filling of solution-synthesized CdS nanowires. *ACS Nano*. 2008, *2*, 357-367.

[34] Protasenko, V. V; Hull, K. L. and Kuno, M; Disorder‐Induced Optical Heterogeneity in Single CdSe Nanowires. *Adv. Mater.* 2005, *24*, 2942-2949.

[35] Glennon, J. J; Tang, R; Buhro, W. E; *et al;* Synchronous photoluminescence intermittency (blinking) along whole semiconductor quantum wires. *Nano Lett.* 2007, *11*, 3290-3295.

[36] Schumacher, T; Giessen, H. and Lippitz, M; Ultrafast Spectroscopy of Quantum Confined States in a Single CdSe Nanowire. *Nano Lett.* 2013, *4*, 1706-1710.